2005

Drag reduction in a flat-plate turbulent boundary layer flow by polymer additives

Shu-Qing Yang
Korea Maritime University, Busan, shuqing@uow.edu.au

G Dou
Nanyang Technological University, Singapore

Drag reduction in a flat-plate turbulent boundary layer flow by polymer additives

Abstract

This paper presents a theoretical study on the velocity distribution and the friction factor of boundary layer flows with polymer additives starting from the concept of “stress deficit.” A novel method of order of magnitude analysis is developed, which converts the governing equations of boundary layer flow into a solvable ordinary differential equation, thus the total shear stress distribution is obtained, then the formulas for the mean velocity profiles and the friction factor for a boundary layer flow are derived after introducing appropriate expressions for the “effective viscosity” and the thickness of viscous sublayer. The derived velocity equation is able to depict the velocity from a solid wall to the outer edge of boundary layer with or without polymer additives using only one fitted parameter D* that is a function of polymer species, its concentration, and Reynolds number. By integrating the velocity profiles, the friction factor and the thickness of boundary layer development are obtained. Experimental data agree well with the theoretical results.

Publication Details

Yang, S. & Dou, G. (2005). Drag reduction in a flat-plate turbulent boundary layer flow by polymer additives. Physics of Fluids, 17 (6), 065104-1-065104-13.

Drag reduction in a flat-plate boundary layer flow by polymer additives

Shu-Qing Yang[a] and G. Dou
Division of Civil and Environmental System Engineering, Korea Maritime University, Busan 606791, Republic of Korea and Maritime Research Centre, Nanyang Technological University, Singapore 639798

(Received 8 July 2004; accepted 7 April 2005; published online 26 May 2005)

This paper presents a theoretical study on the velocity distribution and the friction factor of boundary layer flows with polymer additives starting from the concept of "stress deficit." A novel method of order of magnitude analysis is developed, which converts the governing equations of boundary layer flow into a solvable ordinary differential equation, thus the total shear stress distribution is obtained, then the formulas for the mean velocity profiles and the friction factor for a boundary layer flow are derived after introducing appropriate expressions for the "effective viscosity" and the thickness of viscous sublayer. The derived velocity equation is able to depict the velocity from a solid wall to the outer edge of boundary layer with or without polymer additives using only one fitted parameter D_* that is a function of polymer species, its concentration, and Reynolds number. By integrating the velocity profiles, the friction factor and the thickness of boundary layer development are obtained. Experimental data agree well with the theoretical results. © *2005 American Institute of Physics*. [DOI: 10.1063/1.1924650]

I. INTRODUCTION AND BACKGROUND

It is well known that the addition of a small amount of macromolecular polymer to the Newtonian fluid can lead to dramatic reductions of fluid resistance and form a drag-reduction flow. Such phenomenon, first discovered by Toms,[1] can be utilized to give beneficial effect in engineering and in saving energy resources. Scientists and engineers in the fields of chemistry, physics, and fluid mechanics have hence paid great attention to study it, many experimental and theoretical studies have been carried out to investigate the effects of polymer on a modification of the velocity distributions.

Although this phenomenon has been known for a long time and thousands of research studies and publications have been devoted to the subject over the last 50 years, because of the complexity of the problem, the physical mechanism that causes this drag reduction has still not been clearly identified. The experimental studies on drag reduction flows have been mainly conducted in pipes and channels by researchers such as Virk,[2–4] Seyer and Metzner,[5] James and Acosta,[6] Reischman and Tiederman,[7] Rudd,[8] etc. It has been found from experiments that the drag-reducing effect starts at a certain Reynolds number; below this threshold the flow behaves like a Newtonian fluid, i.e., there is no drag reduction in the flow of dilute polymer solutions, the flow resistance is similar to that of water in the absence of additives and follows the well-known Prandtl–Karman relationship, i.e.,

$$\frac{1}{\sqrt{f}} = 4.0 \log_{10}(\mathrm{Re}\sqrt{f}) - 0.4, \tag{1}$$

in which f is Fanning's friction factor, $2u_*^2/V^2$; $\mathrm{Re}=2Vr/\nu$ where u_* is the shear velocity that is also called "friction" velocity and V is the mean velocity in the flow direction; r is the pipe radius; and ν is the kinematical viscosity of the fluid. In other words, the velocity profile in the absence of drag reduction agent can be expressed by

$$u^+ = y^+, \quad y^+ < 11.6, \tag{2}$$

$$u^+ = 2.5 \ln y^+ + 5.5, \quad y^+ > 11.6, \tag{3}$$

where $u^+ = u/u_*$, $y^+ = u_* y/\nu$, y is the distance from a wall, and u is the streamwise velocity. The viscous-sublayer velocity given by Eq. (2) applies only for $u_* y/\nu < 5$, but often is applied up to its intersection with Eq. (3) at 11.6.

When the Reynolds number is larger than the threshold, it is found that in the turbulent core of polymer solution, the log law is shifted by an amount ΔB, with no change of slope, thus the velocity follows

$$u^+ = 2.5 \ln y^+ + 5.5 + \Delta B. \tag{4}$$

Experiments also show that a dilute polymer solution has a state of maximum drag reduction (MDR). Virk[4] found additionally that all the dilute polymer systems have an asymptotic behavior: Maximum drag reduction is limited by the so-called Virk's MDR asymptote. Virk believed that this asymptote must be a feature of the turbulent flow; it is this hypothesis that makes the drag-reducing effect so extremely interesting from the view point of turbulent research.

Virk[4] proposed that there is an elastic region between the viscous sublayer and the turbulent core, with the ultimate velocity profile that is

$$u^+ = 11.7 \ln y^+ - 17. \tag{5}$$

Virk's three-layer model includes the viscous sublayer, buffer layer, or elastic layer and the turbulent core. In the elastic region, Reischman and Tiederman[7] alternatively suggested that the velocity profile follows

[a]Author to whom correspondence should be addressed. Telephone: 82-51-4104466. Fax: 82-51-4104415. Electronic mail: csqyang@ntu.edu.sg

$$u^+ = 7.687 \ln y^+ - 8. \tag{6}$$

Undoubtedly, dividing the velocity profile of drag-reducing flow into three regions would be useful to empirically express the velocity distribution for the flow of polymer solution. This is probably why Virk's model has been widely adopted by researchers, such as by Larson,[9] Min *et al.*,[10,11] Gasljevic *et al.*,[12] etc.

Turbulent structures in drag-reduction flows have also been observed and reported. Early one-dimensional laser-Doppler-anemometer (LDA) measurement in polymer drag-reducing flows was carried out by Rudd,[8] then followed by Reischman and Tiederman,[7] Berner and Scrivener,[13] Berman,[14] etc. Two-component LDA measurements were conducted by Durst *et al.*,[15] Willmarth *et al.*,[16] Luchik and Tiederman,[17] Harder and Tiederman,[18] Wei and Willmarth,[19] etc. Other researchers[20,21] applied particle image velocimetry (PIV) to a channel flow with polymer additives. These experimental results show that the Reynolds shear stress and the normal velocity fluctuations decrease after a polymer is added. Of particular interest is the existence of "stress deficit" in the drag-reducing flow as reported by Willmarth *et al.*,[16] Gyr and Tsinober,[22] Den Toonder *et al.*,[23] Warholic *et al.*,[20] etc. They found that the total shear stress in drag-reduction flow is greater than the sum of viscous shear stress ($=\nu du/dy$) and the measured Reynolds shear stress ($=-\overline{u'v'}$). Gyr and Tsinober[22] defined the deficit in the following form:

$$G(y) = \frac{\tau}{\rho} - \left[\nu \frac{du}{dy} + (-\overline{u'v'}) \right], \tag{7}$$

where $G(y)$ is the stress deficit, τ is the total shear stress, and $-\overline{u'v'}$ is the Reynolds shear stress.

For turbulent flows of a Newtonian fluid the influence of the viscous shear stress decreases with the wall distance and can be neglected at or above a wall distance of about 80 in viscous units or about 0.15 in distance scaled with the pipe radius,[24] and $G(y)$ must be equal to zero. But for flows with polymer additives, experimental researchers found that $G(y)$ is essentially non-negligible, regardless of pipe flows or boundary layer flows [see Figs. 1(a) and 1(b)]. Typical results from pipe flows are shown in Fig. 1(a), in which the Reynolds shear stress in Newtonian fluid flows denoted by the void symbols was measured by Wei and Willmarth,[19] while the shear stress in flows with polymer additives was measured by Luchik and Tiederman.[17] Min *et al.*[10] used the data shown in Fig. 1(a) to verify the existence of "stress deficit" caused by polymer. Obviously, $G(y)$ can be represented by the difference of measured Reynolds shear stresses shown in Fig. 1(a) when $u_* y/\nu$ is greater than 80. Fontaine *et al.*[25] also observed similar stress deficit phenomenon in a boundary layer flow with polymer injection, the results are presented in Fig. 1(b).

These results indicate that the stress deficit or $G(y)$ is mostly positive due to the elastic effect of polymer; Gyr and Tsinober[22] expressed it as follows:

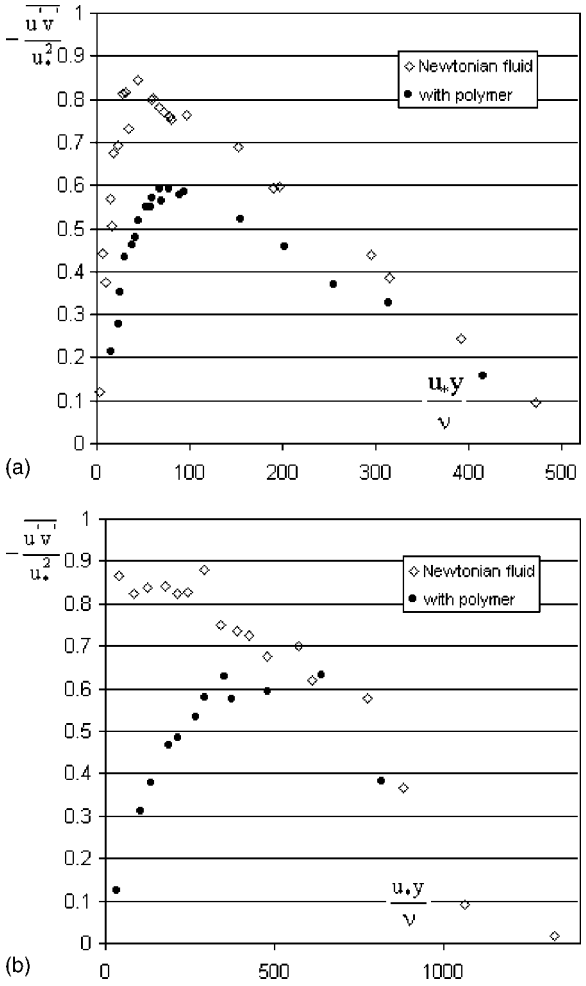

FIG. 1. Measured Reynolds shear stress in Newtonian and drag-reduction flows (a) pipe flow and (b) boundary layer flow.

$$G(y) = \nu_{\text{eff}} \frac{du}{dy}, \tag{8}$$

where ν_{eff} is the effective viscosity. The shear deficit indicates that the viscoelasticity should be the most important property of a dilute polymer solution, the importance of shear deficit shown in Eq. (8) has been realized by direct numerical simulation modelers, such as Min *et al.*[10,11]

It can be seen that the current studies provide valuable insights into polymer drag reduction, yet there still are no available phenomenological equations that can predict the drag reduction by polymer agents. Beginning with the study of Wells and Spangler,[26] it is widely agreed that the polymer must be in the near-wall region for drag reduction to occur. Tiederman *et al.*[27] confirmed experimentally that the drag reduction occurs only when the polymer appears in the region near a boundary, thus the application of polymer drag reduction to boundary layer flows (or a marine system) could be very useful in the theoretical development and practice. Petrie *et al.*[28] reported that the turbulent friction of boundary layer flows could be reduced as much as 60%, thus the drag-reducing applications for ocean-going vessels could potentially result in saving energy resources.

However, the theoretical and experimental attempts made on the velocity distribution and the friction factor in boundary layer flows with polymer additives are extremely lacking relative to pipe/channel flows,[28] except Larson's study[9] in which reasonable conclusions have been obtained but have not been verified by experimental data.

This study deals theoretically with the mean velocity profile and the friction factor of the boundary layer flow with polymer additives, starting from Eq. (7) in which the residual stress or stress deficit caused by polymer additives is expressed by Eq. (8).

The effective viscosity could be approximately related to a characteristic velocity ($=u_*$) and a characteristic length[29] ($=r$), i.e.,

$$\nu_{\text{eff}} = \alpha_* u_* r, \tag{9}$$

where α_* is the apparent viscoelasticity depending on the type of polymer and its concentration. Equation (9) is a phenomenological representation of viscoelastic effects, it may be simplistic relative to numerical simulations, such as those by Min *et al.*,[10,11] Ptasinski *et al.*,[30] Housiadas and Beris,[31] and De Angelis *et al.*,[32] who have indicated a much more complicated mechanism that causes the drag reduction, and these models show that the drag is reduced due to the action of viscoelasticity on modifying the structure of large eddies in the flow. Thus, it is necessary to investigate whether the apparent viscoelasicity α_* is a constant or a function of the distance from the wall ($u_* y/\nu$ or $u_* r/\nu$).

Substituting Eqs. (8) and (9) into Eq. (7), one obtains

$$\frac{\tau}{\rho} = (\nu + \nu_{\text{eff}})\frac{du}{dy} - \overline{u'v'} = \nu D_* \frac{du}{dy} - \overline{u'v'}, \tag{10}$$

where D_* is the drag-reduction parameter, and

$$D_* = 1 + \alpha_* \frac{u_* r}{\nu}. \tag{11}$$

It can be seen that the parameter D_* contains the effects of polymer species, concentration, and Reynolds number.

For a pipe flow, the total shear stress is expressed as $\tau/\rho = u_*^2(1-y/r)$. The main objectives of this study include the following: (1) to obtain the expression of total shear stress in a boundary layer flow, herein a novel method of order of magnitude analysis is developed; (2) to obtain the velocity profile in boundary layer flows with polymer additives by solving the governing equations; (3) to discuss the friction factor and the boundary layer thickness; and (4) to verify the theoretical results with experimental data available in the literature.

II. MEAN VELOCITY DISTRIBUTION

One of the most interesting features in turbulent drag reduction of a dilute polymer solution is the stress deficit, as mentioned above. For a two-dimensional (2D) flow, Min *et al.*[11] derived the total shear stress from an Oldroyd-B model: $\tau = \rho\nu du/dy - \rho\,\overline{u'v'} + \tau_p$ and they termed τ_p as the time averaged stress deficit. It can be seen that τ_p is identical to $G(y)$ in Gyr and Tsinober's expression[22] shown in Eq. (7). Substituting this relationship into the governing equation of boundary layer flow, one has

$$u\frac{\partial u}{\partial x} + v\frac{\partial u}{\partial y} = \nu\frac{\partial^2 u}{\partial y^2} - \frac{\partial \overline{u'v'}}{\partial y} + \frac{\partial \tau_p}{\rho\,\partial y}, \tag{12}$$

$$\frac{\partial u}{\partial x} + \frac{\partial v}{\partial y} = 0, \tag{13}$$

where v is the wall-normal velocity in y direction and x is the streamwise direction.

The boundary conditions are the following: at the bed where $y=0$, $u=v=-\overline{u'v'}=0$; at the outer boundary edge where $y \geqslant \delta$, $u=U_\infty$, $-\overline{u'v'}=\partial u/\partial x=\partial u/\partial y=0$, in which δ is the thickness of the boundary layer; $u=U_\infty$ is the free stream velocity. Thus, the left-hand side (LHS) of Eq. (12) equals zero at $y=0$ and $y=\delta$. Using the boundary conditions the LHS can be approximately expressed as follows:

$$u\frac{\partial u}{\partial x} + v\frac{\partial u}{\partial y} = a_1 y^n (\delta - y)^m, \tag{14}$$

in which a_1 is a coefficient, n and m are exponents to be determined.

Equation (14) shows a way of order of magnitude analysis and it provides a mathematical framework to simplify the governing equation. By analyzing the velocity in laminar flow, we found that the assumption of $n=1.5$ and $m=1$ yields reasonable results for the streamwise and wall-normal velocities (see Tables I and II), this means that the shear stress distribution in a laminar boundary layer flow has been correctly modeled. These exponents, i.e., n and m, could be also extended to the turbulent boundary layer flow with polymer additives, because the profiles of $\tau/\rho u_*^2$ in the laminar and turbulent flows should be similar to each other. This can be seen clearly from the pipe flows, in which the dimensionless shear stresses for both the laminar flow and the turbulent flow with polymer additives obey an identical law, i.e., $\tau/\rho u_*^2 = 1 - y/r$, in other words polymer will not modify the profile of total shear stress, $\tau/\rho u_*^2$. Therefore by substituting Eq. (14) into Eq. (12), one gets

TABLE I. Velocity distribution in laminar boundary layer flows.

$y/\sqrt{x\nu/U_\infty}$	y/δ	Howarth's u_l/U_∞	Equation (39)	Errors (%)	$y/\sqrt{x\nu/U_\infty}$	y/δ	Howarth's u_l/U_∞	Equation (39)	Errors (%)
0	0	0	0		2.8	0.519	0.812	0.805	0.9
0.2	0.037	0.0664	0.0666	0.3	3.0	0.555	0.846	0.840	0.7
0.4	0.074	0.133	0.133	0	3.2	0.593	0.876	0.873	0.3
0.6	0.111	0.199	0.199	0	3.4	0.63	0.902	0.902	0
0.8	0.148	0.265	0.264	0.4	3.6	0.667	0.923	0.926	0.3
1.0	0.185	0.33	0.329	0.3	3.8	0.704	0.941	0.946	0.5
1.2	0.222	0.394	0.391	0.8	4.0	0.741	0.955	0.963	0.8
1.4	0.259	0.456	0.453	0.7	4.2	0.778	0.967	0.976	0.9
1.6	0.296	0.517	0.508	1.7	4.4	0.815	0.976	0.986	1.0
1.8	0.333	0.575	0.569	1.0	4.6	0.852	0.983	0.992	0.9
2.0	0.37	0.63	0.622	1.3	4.8	0.889	0.988	0.997	0.1
2.2	0.407	0.681	0.673	1.2	5.0	0.926	0.992	0.999	0.7
2.4	0.444	0.729	0.720	1.2	5.2	0.963	0.994	0.999	0.5
2.6	0.482	0.772	0.765	0.9	5.4	1	0.996	1	0.4

$$a_1 y^{3/2}(\delta - y) = \frac{\partial}{\partial y}\left(\nu\frac{\partial u}{\partial y} - \overline{u'v'} + \frac{\tau_p}{\rho}\right) = \frac{1}{\rho}\frac{\partial \tau}{\partial y}. \tag{15}$$

Integrating Eq. (15) with respect to y yields

$$\frac{\tau}{\rho} = a_1 y^{7/2}\left(\frac{2}{5}\frac{\delta}{y} - \frac{2}{7}\right) + a_2, \tag{16}$$

where a_2 is an integration constant. At the solid wall where $y=0$, $\tau=\rho u_*^2$, then coefficient a_2 in Eq. (16) is determined as

$$a_2 = u_*^2. \tag{17}$$

At the outer edge of boundary layer where $y=\delta$, $\tau=0$, Eq. (16) gives

$$a_1 = -\frac{35}{4}\frac{u_*^2}{\delta^{3.5}}. \tag{18}$$

Substituting Eqs. (17) and (18) into Eq. (16), one obtains the profile of total shear stress

$$\frac{\tau}{\rho u_*^2} = 1 - \frac{7}{2}\left(\frac{y}{\delta}\right)^{2.5} + \frac{5}{2}\left(\frac{y}{\delta}\right)^{3.5}. \tag{19}$$

Inserting Eq. (10) into (19), one gets

$$\nu D_* \frac{du}{dy} - \overline{u'v'} = u_*^2\left[1 - \frac{7}{2}\left(\frac{y}{\delta}\right)^{2.5} + \frac{5}{2}\left(\frac{y}{\delta}\right)^{3.5}\right]. \tag{20}$$

Similarly, in a turbulent boundary layer flow D_* can be written as $\alpha_* u_* \delta$.

TABLE II. Comparison of Eq. (41) with Howarth's solution on the wall-normal velocity $v\sqrt{x/\nu U_\infty}$ in the laminar boundary layer.

$y/\sqrt{x\nu/U_\infty}$	y/δ	Howarth's $v/\sqrt{\nu U_\infty/x}$	Equation (41)	Errors (%)	$y/\sqrt{x\nu/U_\infty}$	y/δ	Howarth's $v/\sqrt{\nu U_\infty/x}$	Equation (41)	Errors (%)
0	0	0	0		2.8	0.519	0.5206	0.5168	0.71
0.2	0.037	0.0033	0.0033	0.13	3.0	0.555	0.5706	0.5679	0.47
0.4	0.074	0.0132	0.0132	0.02	3.2	0.593	0.6171	0.6193	0.34
0.6	0.111	0.0298	0.0297	0.17	3.4	0.63	0.6595	0.6658	0.96
0.8	0.148	0.0528	0.0525	0.45	3.6	0.667	0.6972	0.7082	1.58
1.0	0.185	0.0821	0.0814	0.78	3.8	0.704	0.7301	0.7458	2.15
1.2	0.222	0.1172	0.1159	1.10	4.0	0.741	0.7581	0.7780	2.62
1.4	0.259	0.1578	0.1556	1.41	4.2	0.778	0.7815	0.8047	2.96
1.6	0.296	0.2032	0.1998	1.67	4.4	0.815	0.8007	0.8255	3.10
1.8	0.333	0.2525	0.2478	1.85	4.6	0.852	0.8160	0.8408	3.04
2.0	0.37	0.3047	0.2988	1.92	4.8	0.889	0.8280	0.8509	2.76
2.2	0.407	0.3588	0.3520	1.88	5.0	0.926	0.8372	0.8565	2.30
2.4	0.444	0.4136	0.4065	1.71	5.2	0.963	0.8441	0.8587	1.73
2.6	0.482	0.4679	0.4628	1.09	5.4	1	0.8491	0.8590	1.17

If, as Dou[33,34] postulated, that, similar to Prandtl's mixing-length theorem, the velocity at an eddy center remains unchanged along a certain distance and the size of eddy follows the Gaussian distribution, then the following Reynolds shear stress is obtained:

$$-\overline{u'v'} = \frac{\kappa}{2}u_* y\frac{\tau}{\rho}\frac{du}{dy} - \frac{\kappa^2}{\delta}(2\delta_* y - y^2)\left(1-\frac{y}{8}\right)\frac{\tau}{\rho}\left(\frac{du}{dy}\right)^2, \qquad (21)$$

where κ is the Karman constant $=0.4$ and δ_* is the thickness of viscous sublayer.

Substituting Eq. (21) into (20), one has

$$\frac{\kappa^2}{8}(2\delta_* y - y^2)\left(1-\frac{y}{\delta}\right)\left[1-\frac{7}{2}\left(\frac{y}{\delta}\right)^{2.5}+\frac{5}{2}\left(\frac{y}{\delta}\right)^{3.5}\right]\left(\frac{du}{dy}\right)^2 - \left\{\frac{\kappa}{2}u_* y\left[1-\frac{7}{2}\left(\frac{y}{\delta}\right)^{2.5}+\frac{5}{2}\left(\frac{y}{\delta}\right)^{3.5}\right]+\nu D_*\right\}\frac{du}{dy} + \left[1-\frac{7}{2}\left(\frac{y}{\delta}\right)^{2.5}+\frac{5}{2}\left(\frac{y}{\delta}\right)^{3.5}\right]u_*^2 = 0. \qquad (22)$$

The velocity gradient du/dy can be determined as follows:

$$\frac{du}{dy} = \frac{\frac{\kappa}{2}u_* y\left[1-\frac{7}{2}\left(\frac{y}{\delta}\right)^{2.5}+\frac{5}{2}\left(\frac{y}{\delta}\right)^{3.5}\right]+\nu D_*}{\frac{\kappa^2}{4}(2\delta_* y - y^2)\left(1-\frac{y}{\delta}\right)\left[1-\frac{7}{2}\left(\frac{y}{\delta}\right)^{2.5}+\frac{5}{2}\left(\frac{y}{\delta}\right)^{3.5}\right]} \times\left[1-\sqrt{1-\frac{\frac{\kappa^2 u_*^2}{2}(2\delta_* y - y^2)\left(1-\frac{y}{\delta}\right)\left[1-\frac{7}{2}\left(\frac{y}{\delta}\right)^{2.5}+\frac{5}{2}\left(\frac{y}{\delta}\right)^{3.5}\right]^2}{\left(\frac{\kappa}{2}u_* y\left[1-\frac{7}{2}\left(\frac{y}{\delta}\right)^{2.5}+\frac{5}{2}\left(\frac{y}{\delta}\right)^{3.5}\right]+\nu D_*\right)^2}}\right]. \qquad (23)$$

Strictly speaking, Eq. (22) is quadratic and has two roots, herein only the root shown in Eq. (23) is discussed because the other root generates unreasonable results. Expressing the square root in Eq. (23) by the Taylor series and keeping only the first three terms, one obtains

$$\frac{du}{dy} = \frac{u_*^2\left[1-\frac{7}{2}\left(\frac{y}{\delta}\right)^{2.5}+\frac{5}{2}\left(\frac{y}{\delta}\right)^{3.5}\right]}{\nu D_* + \frac{\kappa}{2}u_* y\left[1-\frac{7}{2}\left(\frac{y}{\delta}\right)^{2.5}+\frac{5}{2}\left(\frac{y}{\delta}\right)^{3.5}\right]} + \frac{\kappa^2}{8} \times\frac{(2y\delta_* - y^2)(1-y/\delta)^3 u_*^4\left[1-\frac{7}{2}\left(\frac{y}{\delta}\right)^{2.5}+\frac{5}{2}\left(\frac{y}{\delta}\right)^{3.5}\right]^3}{\left\{\nu D_* + \frac{\kappa}{2}u_* y\left[1-\frac{7}{2}\left(\frac{y}{\delta}\right)^{2.5}+\frac{5}{2}\left(\frac{y}{\delta}\right)^{3.5}\right]\right\}^3}. \qquad (24)$$

Equation (24) could be easily integrated, but the result would be too laborious to be used. A simplification could be done as follows: in the near-wall region $1-7(y/\delta)^{2.5}/2+5(y/\delta)^{2.5}/2\approx 1$ for $y\ll\delta$; and in the rest (but $y\neq\delta$), νD_* is very small relative to another term, thus it can be neglected. Therefore, the factor $1-7(y/\delta)^{2.5}/2+5(y/\delta)^{2.5}/2$ in the two terms on the right-hand side of Eq. (24) can be dropped, and Eq. (24) is simplified as

$$\frac{du}{dy} = \frac{u_*^2}{\nu D_* + \frac{\kappa}{2}u_* y} + \frac{\kappa^2}{8}\frac{(2y\delta_* - y^2)(1-y/\delta)u_*^4}{\left(\nu D_* + \frac{\kappa}{2}u_* y\right)^3}. \qquad (25a)$$

Inserting Eq. (25a) into Eq. (20), one obtains the Reynolds shear stress

$$-\frac{\overline{u'v'}}{u_*^2} = 1-\frac{7}{2}\left(\frac{y}{\delta}\right)^{2.5}+\frac{2}{5}\left(\frac{y}{\delta}\right)^{3.5} - \frac{1}{1+\kappa y^+/(2D_*)} - \left(1-\frac{y}{\delta}\right)\frac{\kappa^2}{8D_*^2}\frac{2y^+\delta_*^+ - y^{+2}}{[1+\kappa y^+/(2D_*)]^2}, \qquad (25b)$$

where $\delta_*{}^+ = u_*\delta_*/\nu$.

Integrating Eq. (25a) with respect to y yields

$$\frac{u}{u_*} = \frac{1}{\kappa}\left(1-\frac{2\delta_*^+ + \frac{6D_*}{\kappa}}{\delta^+}\right)\ln\left(1+\frac{\kappa y^+}{2D_*}\right)+\frac{1}{2}\left(\frac{\delta_*^+}{D_*}+\frac{1}{\kappa}\right) \times\left(1+\frac{2D_*}{\kappa\delta^+}\right)\left(\frac{y^+}{2D_*/\kappa + y^+}\right)^2 + \frac{1}{\kappa}\left(1+\frac{2\delta_*^+ + 4D_*/\kappa}{\delta^+}\right) \times\left(\frac{y^+}{2D_*/\kappa + y^+}\right) + \frac{1}{\kappa}\frac{y}{\delta} + c, \qquad (26)$$

where $\delta^+ = u_* \delta / \nu$, c is an integration constant; using the nonslip condition at $y^+ = 0$, $u = 0$, then $c = 0$.

As mentioned above, for Newtonian fluid flows, the actual limit of the viscous sublayer occurs at about $y^+ = 5$, in other words, turbulence affects the velocity distribution in the boundary layer from $y^+ = 5$ outward. However, as commented by Crowe, Elger, and Roberson,[35] the effect is not appreciable up to $y^+ = 11.6$ where the velocity-distribution curves for the viscous sublayer [or Eq. (2)] and the logarithmic velocity distribution [or Eq. (3)] intersect. In derivations and analyses involving the turbulent boundary layers, it is not uncommon to assume that the thickness of viscous sublayer is $\delta_*^+ = u_* \delta_* / \nu = 11.6$.

For turbulent flows with polymer additives, Lumley[36] found that the only difference in the boundary layer turbulence structure between the Newtonian flows and the drag-reducing flows is that polymer molecules are expanded in the flow outside the viscous sublayer due to possible stretching of the polymer molecule (if the strain rate in the turbulent flow is large), this causes an increase in the effective viscosity, which in turn damps dissipative eddies. This effectively leads to a thickening of the viscous sublayer leading to a decrease in the velocity gradient at the wall. Consequently, the Reynolds shear stress at the wall decreases, thus leading to a reduction in the drag.[37] Based on some experimental observations, Dou[38] expressed the thickening of the viscous sublayer with the following relationship:

$$\frac{u_* \delta_*}{\nu} = 11.6 D_*^3. \tag{27}$$

Finally, the mean velocity for drag-reducing boundary layer flow is obtained as follows:

$$\begin{aligned} \frac{u}{u_*} = {} & 2.5\left(1 - \frac{23.2D_*^3 + 15D_*}{\delta^+}\right)\ln\left(1 + \frac{y^+}{5D_*}\right) \\ & + (5.8D_*^2 + 1.25)\left(1 + \frac{5D_*}{\delta^+}\right)\left(\frac{y^+}{5D_* + y^+}\right)^2 \\ & + 2.5\left(1 + \frac{23.2D_*^3 + 10D_*}{\delta^+}\right)\left(\frac{y^+}{5D_* + y^+}\right) \\ & + 2.5\frac{y}{\delta}. \end{aligned} \tag{28}$$

Equation (28) becomes the equation of velocity distribution for Newtonian fluid boundary layer flows when $D_* = 1$.

Similarly, Eq. (25b) can be rewritten as follows:

$$\begin{aligned} -\frac{\overline{u'v'}}{u_*^2} = {} & 1 - \frac{7}{2}\left(\frac{y}{\delta}\right)^{2.5} + \frac{2}{5}\left(\frac{y}{\delta}\right)^{3.5} - \frac{1}{1 + y^+/(5D_*)} \\ & - \left(1 - \frac{y}{\delta}\right)\frac{0.464 y^+ D_* - 0.02(y^+/D_*)^2}{[1 + y^+/(5D_*)]^3}. \end{aligned} \tag{29}$$

Figures 2(a) and 2(b) show the Reynolds shear stress distribution calculated from Eq. (29), in which Klebanoff's experimental data[39] in a Newtonian fluid flow are included for comparison, and good agreements have been achieved. The Reynolds shear stress distribution in the whole boundary layer is shown in Fig. 2(a). However, according to Lumley's theory the presence of walls plays a major role for drag-reducing flows, and the Reynolds shear stress at wall decreases due to the thickening of viscous sublayer, thus the Reynolds shear stress in the near-wall region is particularly plotted in Fig. 2(b) that clearly shows that, as assumed by Lumley[36] and Thirumalai and Bhattacharjee,[37] the Reynolds shear stress at the wall decreases with the increase of D_* or the thickening of viscous sublayer.

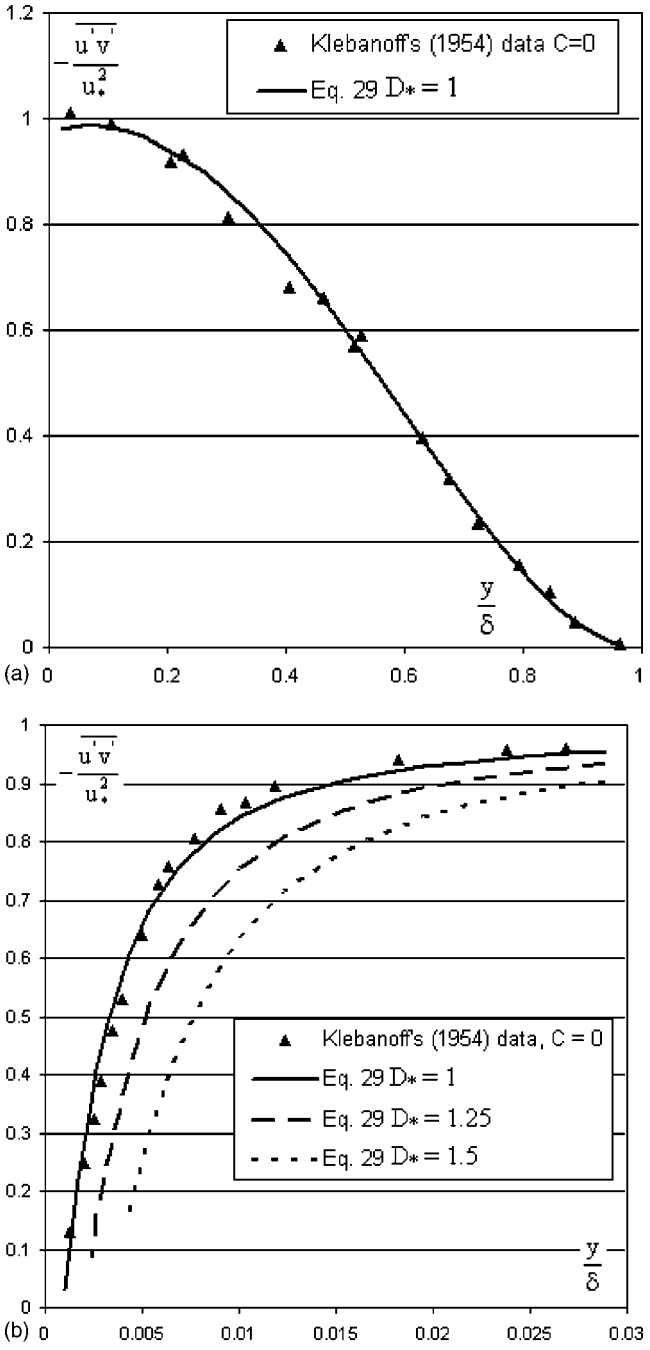

FIG. 2. Reynolds shear stress distribution in boundary layer (a) main flow region and (b) near-wall region.

In the region near the solid wall where $y^+ \ll 5D_*$, one has

$$\ln\left(1 + \frac{y^+}{5D_*}\right) \approx \frac{y^+}{5D_*}; \quad 1 + \frac{y^+}{5D_*} \approx 1;$$

$$\frac{y}{\delta} \approx 0; \quad \left(\frac{y^+}{5D_*}\right)^2 \approx 0;$$

then Eq. (28) becomes

$$\frac{u}{u_*} = \frac{u_* y}{\nu D_*}. \tag{30a}$$

Equation (30a) states that the velocity distribution in the region very near the wall is linear. In the turbulent core where $u_* y/(5\nu D_*) \gg 1$, Eq. (28) can be rewritten as

$$\frac{u}{u_*} = 2.5\left(1 - \frac{23.2D_*^3 + 15D_*}{\delta^+}\right)\ln\left(\frac{y^+}{5D_*}\right) + (5.8D_*^2 + 1.25) \times \left(1 + \frac{5D_*}{\delta^+}\right) + 2.5\left(1 + \frac{23.2D_*^3 + 10D_*}{\delta^+}\right) + 2.5\frac{y}{\delta}. \tag{30b}$$

Equation (30b) states that far away from the boundary, the velocity u/u_* is proportional to the logarithmic distance y^+, its slope and intercept depend on the drag-reduction parameter D_* and $u_*\delta/\nu$. Because $u_*\delta/\nu$ generally is higher than 3000, we take $u_*\delta/\nu = 3000$ as an example; Eq. (30b) can be approximately represented by

$$\frac{u}{u_*} = 2.43 \ln y^+ + 5.7 + \Delta B, \tag{31}$$

where

$$\Delta B = 5.8(D_*^2 - 1) - 2.5 \ln D_*. \tag{32}$$

It can be seen that ΔB in Eq. (4) has been theoretically expressed; it is obvious that ΔB vanishes when $D_* = 1$ or $\alpha_* = 0$.

The free stream velocity U_∞ can be determined from Eq. (28) using the condition $u = U_\infty$ at $y = \delta$,

$$\frac{U_\infty}{u_*} = 2.5 \ln\left(1 - \frac{23.2D_*^3 + 15D_*}{\delta^+}\right)\ln\left(1 + \frac{\delta^+}{5D_*}\right) + (5.8D_*^2 + 1.25)\left(1 + \frac{5D_*}{\delta^+}\right)\left(\frac{\delta^+}{5D_* + \delta^+}\right)^2 + 2.5\left(1 + \frac{23.2D_*^3 + 10D_*}{\delta^+}\right)\left(\frac{\delta^+}{5D_* + \delta^+}\right) + 2.5. \tag{33}$$

The velocity defect can be expressed as

$$\frac{U_\infty - u}{u_*} = 2.5\left(1 - \frac{23.2D_*^3 + 15D_*}{\delta^+}\right)\ln\left(\frac{5D_* + \delta^+}{5D_* + y^+}\right) + (5.8D_*^2 + 1.25)\left(1 + \frac{5D_*}{\delta^+}\right)\left\{\left(\frac{\delta^+}{5D_* + \delta^+}\right)^2 - \left(\frac{y^+}{5D_* + y^+}\right)^2\right\} + 2.5\left(1 + \frac{23.2D_*^3 + 10D_*}{\delta^+}\right) \times \left(\frac{\delta^+}{5D_* + \delta^+} - \frac{y^+}{5D_* + y^+}\right) + 2.5\left(1 - \frac{y}{\delta}\right). \tag{34}$$

In the turbulent core where $y^+ \gg 5D_*$, Eq. (34) can be simplified as

$$\frac{U_\infty - u}{u_*} = 2.5\left(1 - \frac{23.2D_*^3 + 15D_*}{\delta^+}\right)\ln\left(\frac{\delta}{y}\right) + 2.5\left(1 - \frac{y}{\delta}\right) \approx 2.5 \ln\left(\frac{\delta}{y}\right) + 2.5\left(1 - \frac{y}{\delta}\right). \tag{35}$$

It can be seen from Eq. (35) that in the turbulent core the velocity defect depends only on y/δ, and polymer agents have no influence on the velocity defect in this region.

Virk's experimental data[3,4] show that no drag reduction occurs in laminar flows, therefore $D_* = 1$ and $-\overline{u'v'} = 0$. Hence Eq. (20) can be expressed as

$$\nu\frac{du_l}{dy} = u_*^2\left[1 - \frac{7}{2}\left(\frac{y}{\delta}\right)^{5/2} + \frac{5}{2}\left(\frac{y}{\delta}\right)^{7/2}\right], \tag{36}$$

where u_l is the velocity in a laminar flow. Integrating Eq. (36) with respect to y yields

$$\frac{u_l}{u_*} = y^+\left[1 - \left(\frac{y}{\delta}\right)^{5/2} + \frac{5}{9}\left(\frac{y}{\delta}\right)^{7/2}\right]. \tag{37}$$

The relationship between the free stream velocity U_∞ and the thickness of laminar boundary layer δ can be determined from Eq. (37) using the condition $u = U_\infty$ at $y = \delta$,

$$\frac{U_\infty}{u_*} = \frac{5}{9}\frac{u_*\delta}{\nu}, \tag{38}$$

thus, Eq. (37) can be rewritten as follows by introducing Eq. (38):

$$\frac{u_l}{U_\infty} = \frac{9}{5}\left[\frac{y}{\delta} - \left(\frac{y}{\delta}\right)^{7/2} + \frac{5}{9}\left(\frac{y}{\delta}\right)^{9/2}\right]. \tag{39}$$

Equation (39) expresses the velocity distribution of laminar flow in a drag-reducing boundary layer. A comparison of Eq. (39) with the numerical solution of Howarth[29] is shown in Table I, in which $\delta = 5.4(x\nu/U_\infty)^{0.5}$ [see Eq. (51)] is applied. It can be seen from Table I that the maximum relative error of Eq. (39) is only 1.7%, this indicates that Eq. (39) is acceptable to express the velocity for laminar flow of a Newtonian fluid flow, and, by assumption, even when polymer additives are present.

The wall-normal velocity in a laminar boundary flow can be determined from Eq. (13) as follows:

$$\frac{v}{U_\infty} = -\int_0^y \frac{\partial}{\partial x}\left(\frac{u_l}{U_\infty}\right)dy. \tag{40}$$

Substituting Eq. (39) and $\delta = 5.4(x\nu/U_\infty)^{0.5}$ into Eq. (40), one obtains

$$\frac{v}{U_\infty} = \frac{4.86}{\sqrt{U_\infty x/\nu}}\left[\frac{1}{2}\left(\frac{y}{\delta}\right)^2 - \frac{7}{9}\left(\frac{y}{\delta}\right)^{9/2} + \frac{5}{11}\left(\frac{y}{\delta}\right)^{11/2}\right]. \tag{41}$$

Comparison of Eq. (41) with Howarth's numerical solution is shown in Table II.

Table II shows that the maximum relative error of Eq. (41) is only 3.1%. The good agreements shown in Tables I and II indicate that the order assessment and exponents used in Eq. (14), i.e., $n = 1.5$ and $m = 1$, are acceptable.

In the transitional region from the laminar to the turbulent state, Schlichting[29] observed that the velocity profile fol-

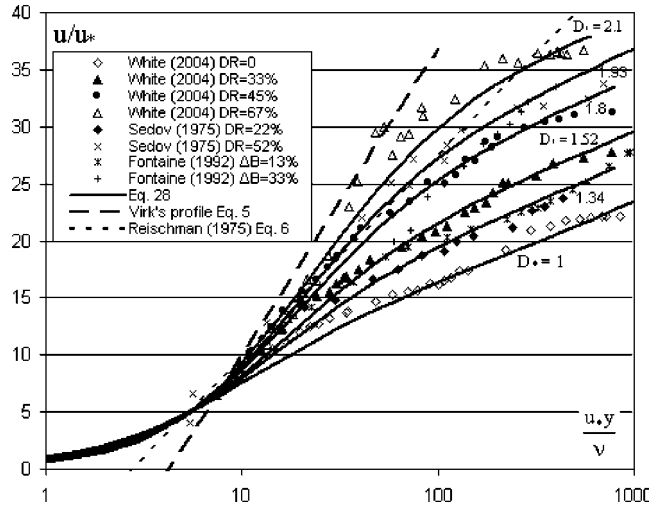

FIG. 3. Comparison of measured velocity distribution in boundary layer flows with polymer additive measured with Eq. (28).

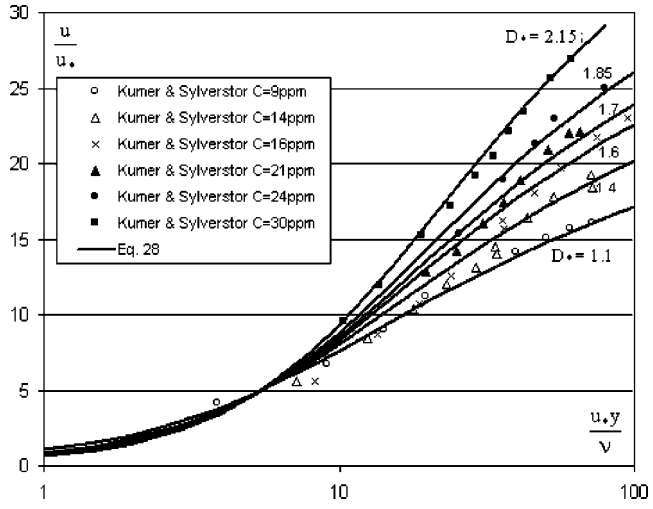

FIG. 4. Comparison of measured velocity distribution in a buffer region with Eq. (28).

lows the law of laminar flow during one period but shifts to the log law during another period; in other words, the velocity profile in the region sometimes corresponds to the laminar distribution and sometimes to the turbulent one, the alternative duration depending on the Reynolds number.[40]

To express the velocity distribution in the region of the laminar to the turbulent transition, Dou[38] suggested

$$\frac{u_t}{u_*} = r_l \frac{u_l}{u_*} + (1 - r_l)\frac{u}{u_*}, \tag{42}$$

where u_t is the velocity in the region of laminar-turbulent transition, u_l is determined by Eq. (37), and u is determined by Eq. (28). The parameter r_l is the probability of laminar occurrences which depends on the relative Reynolds number δ_k^+/δ^+ and can be estimated by the following equation:

$$r_l = \begin{cases} \dfrac{1}{e}\left[\displaystyle\sum_{n=1}^{\infty} \frac{n}{n!}\left(\frac{\delta_k^+}{\delta^+}\right)^{2n}\right] & \text{for } \delta^+ \geqslant \delta_k^+, \\ 1 & \text{for } \delta^+ < \delta_k^+, \end{cases} \tag{43}$$

where δ_k^+ is the critical Reynolds number at which the laminar flow becomes unstable. Therefore the velocity distribution in the transitional region can be determined by Eq. (42) after the velocity profiles in the laminar and fully turbulent regions are determined. It is obvious that when $\delta^+ < \delta_k^+$, $r_l = 1$, Eq. (42) becomes Eq. (37); and when $\delta^+ \gg \delta_k^+$, $r_l = 0$, Eq. (42) becomes Eq. (28), therefore Eq. (42) covers the velocity distributions in laminar, transitional, and turbulent regions.

Figures 3 and 4 show the mean velocity profiles in drag-reducing boundary layer flows measured by White *et al.*,[21] Fontaine *et al.*,[25] Kumor and Sylevstor,[41] and Sedov.[42] White *et al.*[21] conducted the velocity measurement in a water tunnel with a cross sectional dimension of 0.36×0.13 m^2, a PIV system was applied, and the polymer solutions of polyethylene oxide (PEO) with a mean molecular weight of 3.8×10^6 were injected into the boundary layer of flat plate through a spanwise slot 0.15 mm wide located near the leading edge. Fontaine *et al.*[25] measured the velocity profiles in a turbulent boundary layer with slot-injected polymer, laser Doppler velocimeter (LDV) was applied for the experiment, polyethylene oxide solutions were injected, and the polymer averaged molecular weight was 5×10^6, the injection slot was located 0.292 m downstream of the plate leading. Sedov[42] also injected PEO solutions into a flat-plate boundary layer through a slot near the leading edge and the molecular weight of polymer was 0.3×10^6. All these measured velocity profiles are replotted in Fig. 3 in which the drag-reducing parameter D_* is determined by the best fit of measured data when Eq. (28) is applied, the drag reduction (DR) shown in the legend is defined as the ratio of wall shear deficit to the wall shear of flow without polymer injection, ΔB is defined in Eq. (4). In Fig. 3, Virk's[3] and Reischman and Tiederman's[7] ultimate velocity profiles shown in Eqs. (5) and (6), respectively, are also included for comparison. Thus it can be concluded that Eq. (28) is valid in Newtonian and drag-reducing flows. It can be seen that the measured velocity profiles and Eq. (28) are in good agreement, which indicates that the concept of "effective viscosity" proposed by Gyr and Tsinober[22] in Eq. (8) is workable.

In this study, a crucial assumption has been made in Eq. (27) that states $\delta_*^+ = u_* \delta_* \nu = 11.6 D_*^3$. This assumption greatly changes the velocity profile near the bed, particularly the slope in the buffer zone, resulting to a velocity profile that moves upward parallel to the classical logarithmic law of Newtonian fluid flow. It is necessary to check the validity of this assumption using experimental data. Kumor and Sylevstor[41] especially measured the velocity profile in a turbulent boundary layer. They conducted the experiment in a boundary layer flow where the flow of water mixed with POE solutions (concentrations of 9, 14, 16, 21, and 24 ppm) was observed using LDV. As it can be seen from Fig. 4, the measured velocity profiles in the buffer zone agree well with Eq. (28), which indicates that the assumption shown in Eq. (27) is acceptable.

In order to identify whether the drag-reduction parameter D_* is indeed constant or a function of $u_* y/\nu$, the locally determined D_* values versus $u_* y/\nu$ are plotted in Fig. 5(a), in which D_* is obtained in the following method: at a given

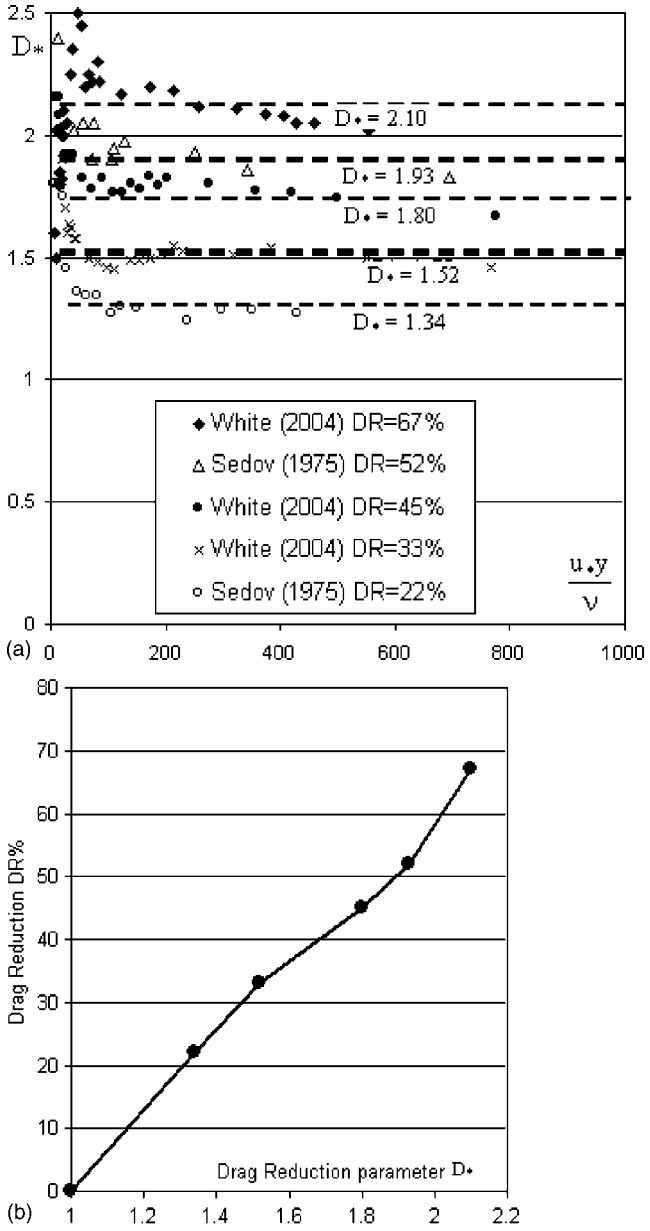

FIG. 5. Relationship between parameter D_* and dimensionless distance u_*y/v (a) and drag reduction DR% (b).

level from the wall, i.e., u_*y/ν, the theoretical velocity in Eq. (28) fully depends on D_*, thus by adjusting the parameter D_*, one can match the theoretical and the measured point velocities.[21,42] Then the obtained D_* versus its location u_*y/ν can be plotted and analyzed. It can be seen that for the region where $u_*y/\nu > 100$, the parameter D_* does not significantly vary with u_*y/ν, in other words D_* can be retreated as a constant in the main flow region. However, Fig. 5(a) also shows that in the near-wall region where $u_*y/\nu < 100$, the calculated D_* is higher than the value obtained from the main flow region. Noticing that for Newtonian fluid flows Eq. (28) does not predict measurement values by White *et al.*[21] in the near-wall region ($u_*y/\nu < 100$) very well (see Fig. 4). One may attribute the variation of D_* in the near-wall region ($u_*y/\nu < 100$) to the systematical error because due to the technical difficulty, the measured velocity near a wall is highly uncertain relative to the measurement in the main flow region. The relationship between the measured drag reduction (DR%) shown in Fig. 5(a) and parameter D_* is shown in Fig. 5(b). As it can be seen there, the drag reduction (DR%) is almost proportional to the drag-reduction parameter D_*.

III. FLOW RESISTANCE

The momentum thickness δ_2 of a flat-plate boundary layer flow is defined as follows:

$$\delta_2 = \int_0^\delta \frac{u}{U_\infty}\left(1 - \frac{u}{U_\infty}\right)dy \tag{44}$$

and the total resistance acting on the plate is expressed as

$$D_{(x)} = \int_0^x \tau_*(x) b dx, \tag{45}$$

where τ_* is the bed shear stress, b denotes the width of the plate; the relationship between the wall shear and the momentum thickness is

$$\tau_*(x) = \rho U_\infty^2 \frac{d\delta_2}{dx}. \tag{46}$$

Inserting Eq. (46) into Eq. (45) yields

$$D_{(x)} = \rho U_\infty^2 \delta_2 b. \tag{47}$$

The dimensionless coefficient for the total skin friction is expressed as

$$c_f = \frac{D_{(x)}}{\frac{\rho}{2} U_\infty^2 x b}. \tag{48}$$

Substituting Eq. (47) into Eq. (48), one obtains

$$c_f = \frac{2\delta_2}{x}. \tag{49}$$

For laminar flow, substituting Eq. (39) into Eq. (44) yields

$$\delta_2 = 0.121\,168\delta. \tag{50}$$

By comparing Eq. (50) with the theoretical result of $\delta_2 = 0.664(x\nu/U_\infty)$, one gets

$$\frac{U_\infty \delta}{\nu} = 5.4\sqrt{\frac{U_\infty x}{\nu}}. \tag{51}$$

Inserting Eqs. (50) and (51) into Eq. (49), one has

$$c_f = \frac{1.3085}{\sqrt{U_\infty x/\nu}}. \tag{52a}$$

Equation (52a) is the friction factor in laminar flows which is very close to the theoretical results:[29]

$$c_f = \frac{1.328}{\sqrt{U_\infty x/\nu}}. \tag{52b}$$

For fully turbulent flows in the flat-plate boundary layer with polymer additive, the friction factor c_f can be determined

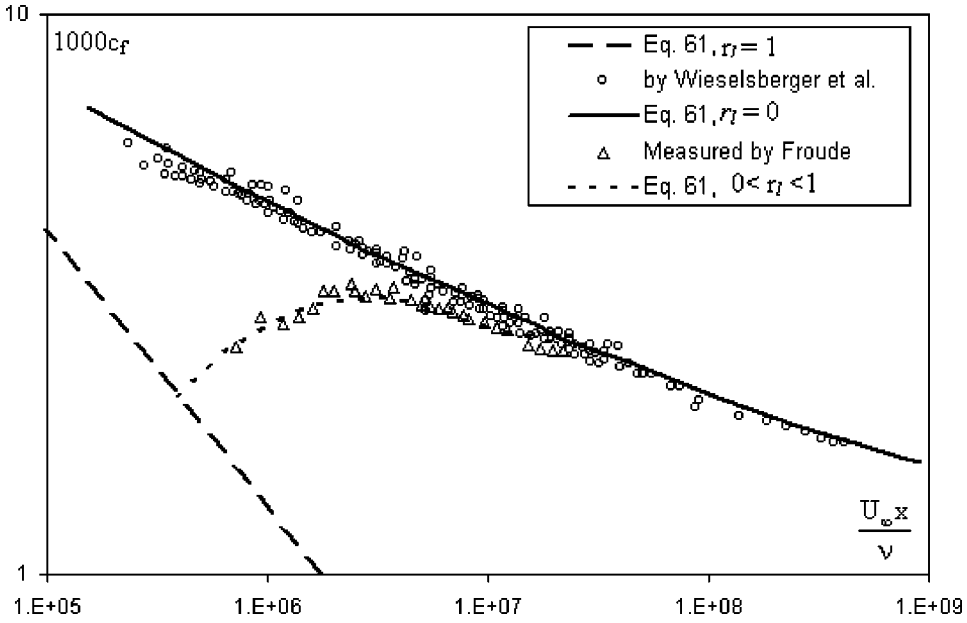

FIG. 6. Skin friction coefficient vs Reynolds number for the boundary layer of a Newtonian fluid ($D_*=1$ or $\alpha_*=0$) and data from Schlichting (Ref. 29).

using the similar way mentioned, and Eq. (44) can be written in a dimensionless form

$$\frac{U_\infty \delta_2}{\nu} = \int_0^{\delta^+} \frac{u}{u_*} dy^+ - \int_0^{\delta^+} \left(\frac{u}{u_*}\right)^2 \Big/ \left(\frac{U_\infty}{u_*}\right) dy^+. \tag{53}$$

Let $f_1(\delta^+)=U_\infty/u_*$; $f_2(\delta^+)=\int_0^{\delta^+}(u/u_*)dy^+$; $f_3(\delta^+)=\int_0^{\delta^+}(u/u_*)^2 dy^+$. Equation (53) can be rewritten as follows:

$$\frac{U_\infty \delta_2}{\nu} = f_2(\delta^+) - f_3(\delta^+)/f_1(\delta^+). \tag{54}$$

From Eq. (46), the relationship for x and δ^+ can be derived,

$$x = \int_0^{\delta^+} f_1^2(\delta^+) \frac{d\delta_2}{d\delta^+} d\delta^+. \tag{55}$$

$d\delta_2/d\delta^+$ can be determined from Eq. (54) in the following form:

$$\frac{d\left(\frac{U_\infty \delta_2}{\nu}\right)}{d\delta^+} = \frac{f_3(\delta^+)}{f_1^2(\delta^+)} \frac{df_1(\delta^+)}{d\delta^+}. \tag{56}$$

Inserting Eq. (56) into Eq. (55), one obtains

$$\frac{U_\infty x}{\nu} = f_3(\delta^+) f_1(\delta^+) - \int_0^{\delta^+} f_3'(\delta^+) f_1(\delta^+) d\delta^+ \tag{57}$$

for

$$f_3'(\delta^+) = f_1^2(\delta^+), \tag{58}$$

therefore, one has

$$\frac{U_\infty x}{\nu} = f_3(\delta^+) f_1(\delta^+) - f_4(\delta^+), \tag{59}$$

where

$$f_4(\delta^+) = \int_0^{\delta^+} \left(\frac{U_\infty}{u_*}\right)^3 d\delta^+. \tag{60}$$

Inserting Eqs. (54) and (59) into Eq. (49), one obtains the formula of friction factor for the boundary layer flows,

$$c_f = 2\frac{f_2(\delta^+) - f_3(\delta^+)/f_1(\delta^+)}{f_1(\delta^+) f_3(\delta^+) - f_4(\delta^+)}. \tag{61}$$

The free stream velocity U_∞/u_* in f_1 and f_4 can be obtained from Eqs. (33), (39), and (42) as follows:

$$\frac{U_\infty}{u_*} = r_l \frac{5}{9}\delta^+ + (1-r_l)\left\{2.5\left(1 - \frac{23.2D_*^2 + 15}{\delta^+}\right)\ln\left(1 + \frac{\delta^+}{5}\right) + (5.8D_*^2 + 1.25)\left(1 + \frac{5}{\delta^+}\right)\left(\frac{\delta^+}{5+\delta^+}\right)^2 + 2.5\left(1 + \frac{23.2D_*^2 + 10}{\delta^+}\right)\left(\frac{\delta^+}{5+\delta^+}\right) + 2.5\right\}, \tag{62}$$

where, when the flow is laminar, $r_l=1$; and in the fully de-

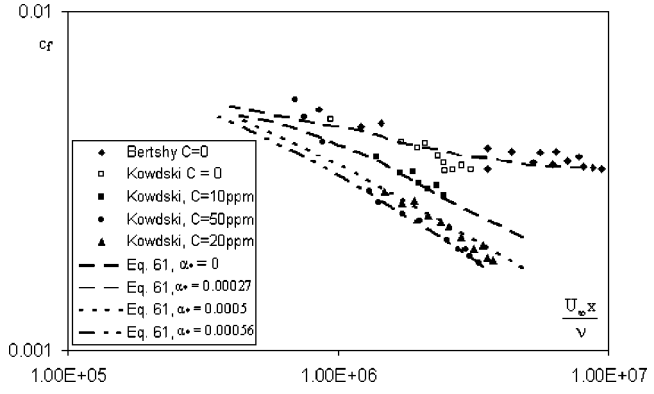

FIG. 7. Skin friction coefficient vs Reynolds number for the boundary layer flow with polymer additives ($\alpha_*>0$) and data from Sedov (Ref. 41).

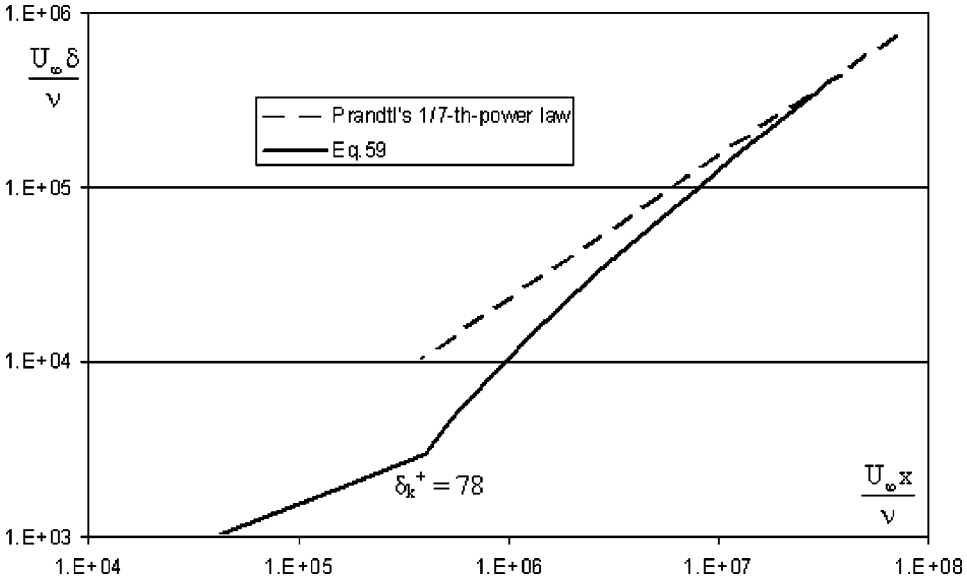

FIG. 8. Boundary layer thickness development in a Newtonian fluid boundary layer.

veloped turbulent region, $r_l=0$; in the laminar-turbulent transition, $0<r_l<1$.

The mean velocity u/u_* in f_2 and f_3 can be determined using the aforementioned equations, i.e., Eq. (42). Thus one is able to calculate the friction factor c_f using Eq. (61) numerically, and the obtained results can cover the laminar, transitional, and fully turbulent flow regions for both Newtonian and drag-reducing fluid flows because Eqs. (42) and (62) can cover these three regions.

A comparison between Eq. (61) and the measured data is shown in Fig. 6 in Newtonian fluid boundary layer flows, in which the experimental data were collected by Schlichting,[29] the theoretical results shown in Fig. 6 are calculated on the basis of three input conditions, i.e., $r_l=0$ (full turbulence); $r_l=1$ (fully laminar status); and $0<r_l<1$. For the condition $0<r_l<1$, the critical Reynolds number ($\delta_k^+=78.4$ or $U_\infty x/\nu = 400\,000$) is assumed and r_l is calculated using Eq. (43). It can be seen from Fig. 6 that the predicted skin friction for Newtonian fluids is in good agreement with experiments over a wide range of Reynolds number. Larson[9] conducted a similar study. His model can also provide a reasonable agreement with Schlichting's data[29] over a range of Reynolds number spanning from 10^5 to 10^9, but his model cannot predict the skin friction in the laminar-turbulent transition.

Equation (61) is then applied to the turbulent boundary layer flows ($r_l=0$) with polymer additives; the results are shown in Fig. 7, in which the experimental data were compiled by Sedov.[42]

Figure 7 shows clearly that with increasing polymer concentration the friction coefficient is reduced gradually, and the theoretical results and the experimental data are in good agreement.

The boundary thickness development in a Newtonian fluid flow is calculated using Eq. (59). The obtained $U_\infty \delta/\nu$ versus $U_\infty x/\nu$ is plotted in Fig. 8; in the calculation the critical Reynolds number δ_k^+ is equal to 78, similar to that in Fig.

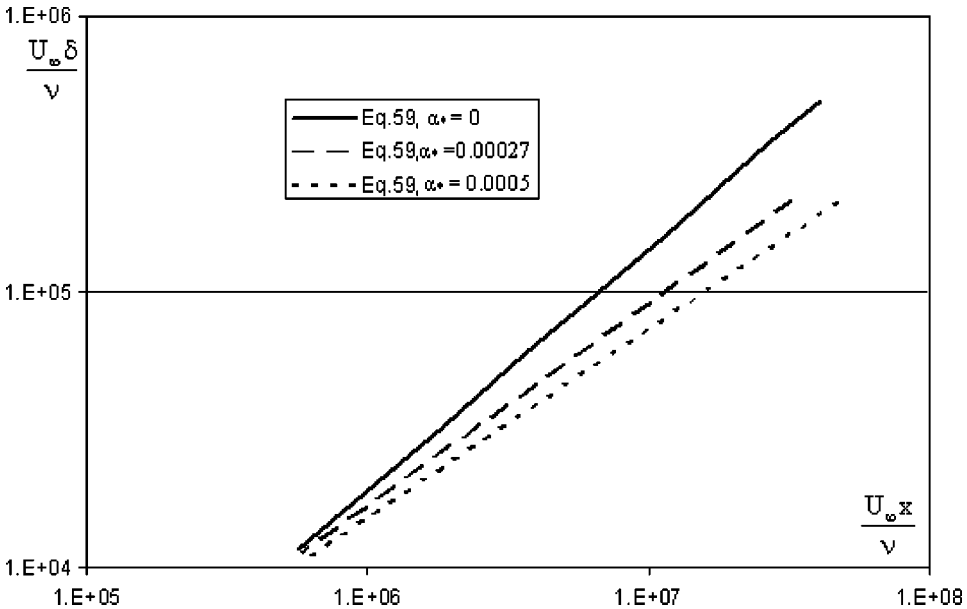

FIG. 9. Comparison of boundary layer thickness development in drag-reduction flow.

6, this value is also used to calculate the probability r_l. The theoretical results show that near the leading edge, the Reynolds number is less than the critical Reynolds number and the flow is laminar, thus Eq. (51) can be used for the calculation. As the Reynolds number increases, the flow becomes unstable in the region of laminar-turbulent transition. It is seen from Fig. 8 that the calculated results gradually approach their asymptote—the well-known Prandtl's 1/7th-power law—i.e., $U_\infty \delta/\nu = 0.38(U_\infty x/\nu)^{0.8}$; this indicates that Eq. (51) is reasonable and also implies that Prandtl's law is invalid when $U_\infty x/\nu < 8\times 10^7$.

The boundary thickness development in drag-reduction flows is shown in Fig. 9. The drag-reduction parameter α_* obtained from Fig. 7 is used in the calculation. It can be seen that with the increment of parameter α_*, the boundary thickness $U_\infty \delta/\nu$ becomes thinner relative to Newtonian fluid flows, the conclusion is consistent with Larson's study.[9]

IV. CONCLUSIONS

By applying the concept of stress deficit and developing a novel method of order of magnitude analysis for a drag-reducing boundary layer flow, the formulas for mean velocity, friction factor, and boundary layer thickness are obtained. The theoretical results are in good agreement with the measured data available in the literature using only one fitting parameter D_* that is a function of polymer species, its concentration, and Reynolds number. The following conclusions can be drawn from the study.

(1) The stress deficit can be assumed to be proportional to the velocity gradient and the effective viscosity; the latter can be expressed in a form similar to the eddy viscosity. The parameter D_* obtained from the concept of stress deficit increases linearly with Reynolds number.
(2) The velocity profile in drag-reducing boundary layer flows can be divided into three zones as Virk[3] did, i.e., viscous sublayer, buffer zone, and turbulence core, but the velocity profile in these three zones can be expressed by Eq. (28). In the buffer zone the slope of velocity profile in a semilogarithmic plot is variable, but in the turbulent core, the slope is constant though its intercept moves upward by an amount of ΔB. This study gives a theoretical expression of ΔB that is only related to the parameter D_*. A good agreement between the measured and predicted velocity profiles is achieved using the fitted parameter D_*.
(3) Based on the theoretical velocity profile developed in this study, the formula for friction factor in a boundary layer flow is derived, which covers the friction factor in laminar, laminar-turbulent transition, and fully turbulent flows. It provides a good agreement with the experimental data using only one fitted parameter.
(4) The development of boundary layer thickness has been numerically calculated. The results show that near the leading edge of a flat plate, the boundary layer is laminar. It is found that the boundary layer thickness gradually approaches its asymptote—the well-known Prandtl's 1/7th-power law—but Prandt's law overestimates the boundary layer thickness when the Reynolds number is less than 8×10^7.
(5) This study shows that the introduction of polymer in a Newtonian fluid flow attenuates the thickness of boundary layer relative to that in a Newtonian fluid flow.

[1] B. A. Toms, "Some observation on the flow of linear polymer solutions through straight tubes at large Reynolds numbers," *Proceedings of the First International Congress on Rheology, 1949*.
[2] P. S. Virk, "The Toms phenomenon," J. Fluid Mech. **30**, 305 (1967).
[3] P. S. Virk, "An elastic sublayer model for drag reduction by dilute solutions of linear macromolecules," J. Fluid Mech. **45**, 417 (1971).
[4] P. S. Virk, "Drag reductions in rough pipes," J. Fluid Mech. **45**, 225 (1971).
[5] F. A. Seyer and A. B. Metzner, "Turbulence phenomena in drag reducing systems," AIChE J. **5**, 426 (1969).
[6] D. F. James and A. J. Acosta, "The laminar flow of dilute polymer solutions around circular cylinders," J. Fluid Mech. **42**, 269 (1970).
[7] M. M. Reischman and W. G. Tiederman, "Laser-Doppler-anemometer measurements in drag-reducing channel flows," J. Fluid Mech. **70**, 369 (1975).
[8] M. J. Rudd, "Velocity measurements made with a laser Dopplermeter on the turbulent pipe flow of a dilute polymer solution," J. Fluid Mech. **51**, 673 (1972).
[9] R. G. Larson, "Analysis of polymer turbulent drag reduction in flow past a flat plate," J. Non-Newtonian Fluid Mech. **111**, 229 (2003).
[10] T. Min, H. Choi, and J. Y. Yoo, "Maximum drag-reduction in a turbulent channel flow by polymer additives," J. Fluid Mech. **492**, 91 (2003).
[11] T. Min, J. Y. Yoo, H. Choi, and D. D. Joseph, "Drag reduction by polymer additives in a turbulent channel flow," J. Fluid Mech. **486**, 213 (2003).
[12] K. Gasljevic, G. Aguilar, and E. F. Matthys, "On two distinct types of drag-reducing fluids, diameter scaling, and turbulent profiles," J. Non-Newtonian Fluid Mech. **96**, 405 (2001).
[13] C. Berner and O. Scrivener, "Drag reduction and structure of turbulence in dilute polymer solutions," in *Viscous Flow Drag Reduction*, Progress in Astronautics and Aeronautics, Vol. 72, edited by G. R. Hough (AIAA, New York, 1979), p. 290
[14] N. S. Berman, "Velocity fluctuations in non-homogeneous drag reduction," Chem. Eng. Commun. **42**, 37 (1986).
[15] F. Durst, T. Keck, and R. Kline, "Turbulence quantities and Reynolds stresses in pipe flow of polymer solutions," *Proceedings of the First International Conference on Laser Anemometer—Advances and Applications, BHRA, 1985*.
[16] W. W. Willmarth, T. Wei, and C. O. Lee, "Laser anemometer measurements of Reynolds stress in a turbulent channel flow with drag reducing polymer additives," Phys. Fluids **30**, 933 (1987).
[17] T. S. Luchik and W. G. Tiederman, "Turbulent structure in low-concentration drag-reducing channel flows," J. Fluid Mech. **190**, 241 (1988).
[18] K. J. Harder and W. G. Tiederman, "Drag reduction and turbulent structure in two-dimensional channel flows," Philos. Trans. R. Soc. London, Ser. A **336**, 19 (1991).
[19] T. Wei and W. W. Willmarth, "Modifying turbulent structure with drag-reducing polymer additives in turbulent channel flows," J. Fluid Mech. **245**, 619 (1992).
[20] M. D. Warholic, H. Massah, and T. J. Hanratty, "Influence of drag-reducing polymers on a turbulence: Effects of Reynolds number, concentration and mixing," Exp. Fluids **27**, 461 (1999).
[21] C. M. White, V. S. R. Somandepalli, and M. G. Mungal, "The turbulence structure of drag-reduced boundary layer flow," Exp. Fluids **36**, 62 (2004).
[22] A. Gyr and A. Tsinober, "On the rheological nature of drag reduction phenomena," J. Non-Newtonian Fluid Mech. **73**, 153 (1997).
[23] J. M. J. Den Toonder, M. A. Hulsen, G. D. C. Kuiken, and F. T. M. Nieuwstadt, "Drag reduction by polymer additives in a turbulent pipe flow: Numerical and laboratory experiments," J. Fluid Mech. **337**, 193 (1997).
[24] A. Gyr and H.-W. Bewersdorff, *Drag Reduction of Turbulent Flows by Additives* (Kluwer Academic, Boston, 1995).
[25] A. A. Fontaine, H. L. Petrie, and T. A. Brungart, "Velocity profile statistics in a turbulent boundary layer with slot-injected polymer," J. Fluid Mech. **238**, 435 (1992).

[26]C. S. Wells and J. G. Spangler, "Injection of drag-reducing fluid into a turbulent pipe flow of a Newtonian fluid," Phys. Fluids **10**, 1890 (1967).
[27]W. G. Tiederman, T. S. Luchik, and D. G. Bogard, "Wall-layer structure and drag reduction," J. Fluid Mech. **156**, 419 (1985).
[28]H. L. Petrie, S. Deutsch, T. A. Brungart, and A. A. Fontaine, "Polymer drag reduction with surface roughness in flat-plate turbulent boundary layer flow," Exp. Fluids **35**, 8 (2003).
[29]H. Schlichting, *Boundary Layer Theory* (McGraw-Hill, New York, 1979), p. 639.
[30]P. K. Ptasinski, B. J. Boersma, F. T. M. Nieuwstadt, M. A. Hulsen, B. H. A. A. Van den Brule, and J. C. R. Hunt, "Turbulent channel flow near maximum drag reduction: Simulations, experiments and mechanisms," J. Fluid Mech. **490**, 251 (2003).
[31]K. D. Housiadas and A. N. Beris, "Polymer-induced drag reduction: Effects of the variations in elasticity and inertia in turbulent viscoelastic channel flow," Phys. Fluids **15**, 2369 (2003).
[32]E. De Angelis, C. M. Casciola, and R. Piva, "DNS of wall turbulence: Dilute polymers and self-sustaining mechanisms," Comput. Fluids **31**, 495 (2002).
[33]G. R. Dou, "Turbulent structure in open channels and pipes," Sci. Sin. **24**, 727 (1981).
[34]G. R. Dou, *Mechanics of Turbulent Flows* (The People's Education, Beijing, China, 1982) (in Chinese).
[35]C. T. Crowe, D. F. Elger, and J. A. Roberson, *Engineering Fluid Mechanics*, 7th ed. (Wiley, New York, 2001).
[36]J. L. Lumley, "Drag-reduction by additives," Annu. Rev. Fluid Mech. **1**, 367 (1969).
[37]D. Thirumalai and J. K. Bhattacharjee, "Polymer-induced drag reduction in turbulent flows," Phys. Rev. E **53**, 546 (1996).
[38]G. R. Dou, "Basic law in mechanics of turbulent flows," China Ocean Engineering **10**, 1 (1996).
[39]P. S. Klebanoff, "Characteristics of turbulence in a boundary layer with zero pressure gradient," Natl. Advisory Comm. Aeronaut. Tech. Report No. 3178, 1954.
[40]A. A. Draad, G. D. C. Kuiken, and F. T. M. Nieuwstadt, "Laminar-turbulent transition in pipe flow for Newtonian and non-Newtonian fluids," J. Fluid Mech. **377** 267 (1998).
[41]S. M. Kumor and N. D. Sylevstor, "Effect of a drag reduction polymer on the turbulent boundary layer," AIChE Symp. Ser. **2**, 134 (1973).
[42]V. T. Sedov, "Calculation of turbulent boundary layers with polymer additive," *Proceedings of the International Conference on Drag Reduction*.